Enhanced Apoptosis in Choroidal Tissues in Lens-Induced Myopia Guinea Pigs by Activating the RASA1 Signaling Pathway

Jinpeng Liu,[1] Huixia Wei,[2] Zhaohui Yang,[1] Yixian Hao,[2] Guimin Wang,[2] Tuling Li,[1] Ting Yu,[1] Huiping Liao,[1] Bo Bao,[1] Qiuxin Wu,[2] Hongsheng Bi,[2] and Dadong Guo[3]

[1]Shandong University of Traditional Chinese Medicine, Jinan, China
[2]Affiliated Eye Hospital of Shandong University of Traditional Chinese Medicine, Jinan, China
[3]Shandong Provincial Key Laboratory of Integrated Traditional Chinese and Western Medicine for Prevention and Therapy of Ocular Diseases, Shandong Academy of Eye Disease Prevention and Therapy, Medical College of Optometry and Ophthalmology, Shandong University of Traditional Chinese Medicine, Jinan, China

Correspondence: Dadong Guo, Shandong Academy of Eye Disease Prevention and Therapy, Medical College of Optometry and Ophthalmology, Shandong University of Traditional Chinese Medicine, No. 48, Yingxiongshan Road, Jinan, Shandong 250002, China;
dadonggene@163.com.
Hongsheng Bi, Shandong Academy of Eye Disease Prevention and Therapy, Affiliated Eye Hospital of Shandong University of Traditional Chinese Medicine, No. 48, Yingxiongshan Road, Jinan, Shandong 250002, China;
azuresky1999@163.com.

PURPOSE. This study aimed to explore the role of the RAS p21 protein activator 1 (RASA1) signaling pathway in apoptosis in choroid tissues from guinea pigs with negative lens-induced myopia (LIM).

METHODS. Biometric measurements were performed to examine refractive status, ocular parameters, and choroidal thickness (ChT) after myopia induction. The choroidal morphology was observed by hematoxylin and eosin (H&E) staining and TUNEL assay. The expression of the RASA1 signaling pathway at the mRNA and protein levels in choroidal tissues was measured by real-time quantitative PCR (qPCR) and western blot assays.

RESULTS. Compared with the normal control (NC) group, the ocular length of the guinea pigs in LIM increased remarkably, as did the myopic refraction. ChT decreased after myopia induction. H&E staining showed that the thickness and laxity of the choroidal tissues in LIM were strikingly reduced. The number of apoptotic cells in the LIM eyes was increased. Moreover, qPCR and western blot assays showed that the expression levels of both *RASA1* and BCL-2-associated agonist of cell death (*BAD*) were higher in the LIM group than in the NC group, whereas the expression level of B-cell lymphoma 2 (*BCL-2*) was decreased after 2 weeks of experimental myopia. However, the trend of RASA1, BAD, and BCL-2 expression was reversed after 4 weeks of experimental myopia compared with levels after 2 weeks of experimental myopia.

CONCLUSIONS. Results showed that the RASA1 signaling pathway is activated in choroid tissues in myopic guinea pigs. Activated RASA1 signaling induces high BAD expression and low BCL-2 expression, which in turn promotes apoptosis and ultimately causes ChT thinning in myopic guinea pigs.

Keywords: RASA1 signaling pathway, lens-induced myopia, choroidal thickness, BCL-2, apoptosis

Currently, myopia incidence is increasing worldwide, and it has grown to alarming levels in East Asian countries.[1] Based on an epidemiological survey, the prevalence of myopia in adolescents is approximately 80% to 90% in East Asian countries.[2] Due to changing lifestyles (such as less time spent outdoors and more near work/reading), the incidence of myopia is increasing each year.[3,4] In fact, myopia is one of the common eye diseases in China.[5] An investigation revealed that the incidence of myopia among Chinese students is nearly 50% among primary and secondary school students.[6,7] Both environmental and genetic factors contribute to myopia development. Studies pertaining to environmental factors have identified indoor activities and near work as risk factors of myopia, whereas genetic studies have shed light on various candidate genes and genetic loci associated with myopia.[8,9]

The complications of high myopia can lead to serious visual impairment, and the most significant and common complications are atrophic myopic macular degeneration/retinopathy and even blindness. However, the pathogenesis of myopia remains unclear.[10] The choroid is a subretinal layer of the retina that can provide metabolic support for the retinal pigment epithelium, provide blood supply for the outer retina, and participate in lymphatic drainage.[11] Currently, we recognize that the choroid is a five-layered structure consisting (from the outside to the inside) of the basement membrane of the choriocapillaris, outer collagenous zone, elastic layer, inner collagenous zone, and basement membrane of the retinal pigment epithelium. The choroid is composed of blood vessels, melanocytes, fibroblasts, resident immune cells, and supporting collagen and elastic connective tissue. Furthermore, in addition to

the five layers of structure described above, the choroidal interstitium contains collagen and elastic fibers, fibroblasts, nonvascular smooth muscle cells, and numerous very large melanocytes that are closely apposed to the blood vessels. As in other types of connective tissue, there are numerous mast cells, macrophages, and lymphocytes.[12] As the most important supply tissue, the choroid supplies blood to the prelaminar portion of the optic nerve and absorbs excessive light penetrating the retina.[12,13] The central retinal artery supplies the inner part of the retina, and the choroidal venous network supplies the remaining third of the outer part. Abnormal choroidal blood flow leads to retinal photoreceptor dysfunction and photoreceptor death[14]; thus, the choroid plays an important role in the pathophysiology of myopia. In addition, it has been shown that choroidal blood flow plays an important role in the development of myopia, not only by providing abundant blood flow to the fundus but also by acting as a signal transduction pathway between the retina and the sclera, thereby mediating the development of myopia.[15]

RAS P21 protein activator 1 (RASA1) is an essential RAS GTPase-activating protein that can negatively regulate RAS activity by elevating the rate of guanosine triphosphate (GTP) hydrolysis.[16] Additionally, RASA1 can also function as a signal transducer and transcription regulator.[17] It has also been confirmed that RASA1 signaling is closely related to angiogenesis, cellular growth, cell proliferation, fibrosis, and apoptosis.[18,19] To investigate the role of RASA1 signaling-related molecules in the choroid in the development of lens-induced myopia (LIM), we established the LIM model in guinea pigs with −6.0 diopter (D) lenses covering the right eye. After 2 and 4 weeks of myopia induction, we isolated choroidal tissues to observe morphological changes, determine the levels of RASA1 signaling-related molecules, and measure choroidal thickness (ChT). The current study aimed to elucidate the relationship between choroidal tissues and the development of myopia, thus providing evidence for the underlying mechanism of the development of myopia.

MATERIALS AND METHODS

Animals

The present study was approved by the Ethics Committee of Shandong University of Traditional Chinese Medicine and adhered to the ARVO Statement for the Use of Animals in Ophthalmic and Vision Research. Prior to enrollment, guinea pigs with various ocular conditions, including cataracts and corneal disease, were excluded. In the present study, 42 healthy 2-week-old guinea pigs (_Cavia porcellus_, English short-hair stock, tricolor strain; Danyang Changyi Experimental Animal Company, Jiangsu, China) with a mean weight between 100 and 120 g were chosen for the relevant experiments. The guinea pigs were then divided into a normal control (NC) group (_n_ = 21) and a LIM group (_n_ = 21) using the random number table method. The guinea pigs were raised at a constant temperature of 25°C ± 2°C with humidity ranging from 40% to 70%; noise levels were less than 60 dB. The experiments were conducted with natural light during the daytime, with a 12 hour/12 hour light/dark cycle and a light intensity of 500 lux in the cage.[20]

Preparation of the LIM Guinea Pig Model

Refractive and other ocular measurements were measured prior to myopia induction. In the present study, we used

−6.0 D spherical resin lenses to establish the LIM model.[21] The right eyes of guinea pigs in the LIM group were covered with a −6.0 D lens to induce myopia for 2 and 4 weeks, whereas both eyes of the animals in the NC group were left untreated. During myopia induction, when any lenses fell off they were promptly reattached. To ensure the validity of the LIM model in guinea pigs, all lenses were cleaned and wiped every morning and evening and replaced promptly if there were obvious scratches.

Biometric Measurements

After 2 and 4 weeks of myopia induction, refractive error was measured for animals from both the NC and LIM groups. Prior to the examination, the lenses covered on the eyes of guinea pigs were gently removed with scissors, and 10 mg/mL of cyclopentolate hydrochloride eye drops (Alcon, Geneva, Switzerland) was dropped into the conjunctival capsule of the guinea pigs three times, one drop each time, at an interval of 5 minutes. Refractive examinations were performed 30 to ~45 minutes after the last eye drop application. Each eye was measured at least six times, and the average value was taken as the experimental result. Ophthalmic A-type ultrasonography (Cinescan; Quantel Medical, Cournon-d'auvergne, France) was used for the measurement of ocular axis length. Then, two drops of oxybuprocaine hydrochloride (Santen Pharmaceutical, Osaka, Japan) were administered, with one drop each time before measurement. Topical anesthetic (Santen Pharmaceutical) was administered before measuring ocular length. The anterior chamber propagation velocity was 1557 m/s, the lens propagation velocity was 1723 m/s, and the vitreous propagation velocity was 1540 m/s. A total of 10 readings were averaged to serve as the final one, as described previously.[22]

Histopathological Staining and TUNEL Assay

Three guinea pigs in each group were randomly selected at 4 weeks of myopia induction for histopathological staining. Guinea pigs were euthanized with an intraperitoneal injection of 4% pentobarbital followed by enucleation of the eye and removal of periocular tissues. The eyeball was immediately fixed in 4% paraformaldehyde, followed by conventional dehydration, paraffin embedding, and sectioning into 5-μm sections for hematoxylin and eosin (H&E) staining.[23]

Briefly, paraffin sections of the eye tissues were dewaxed, treated with proteinase K, and then incubated at 37°C for 20 minutes. Subsequently, the sections were quenched in 3% hydrogen peroxide solution, incubated with terminal deoxynucleotidyl transferase, and labeled with biotin–dUTP labeling mix for the apoptotic DNA fragments. Furthermore, the sections were subjected to chromogenic detection and hematoxylin restaining using diaminobenzidine (DAB) chromogenic solution.[24] Finally, the sections were observed using light microscopy (Eclipse 55i; Nikon, Tokyo, Japan) and analyzed using NIS-Elements D 3.2 software (Nikon).

Measurement of ChT

We used spectral-domain OCT (Heidelberg Engineering, Heidelberg, Germany) and OCT to scan the optic disc center of the guinea pigs to obtain the relevant parameter of ChT. As illustrated in Figure 1, the upper boundary of the choroid was defined as the outer surface of the retinal pigment
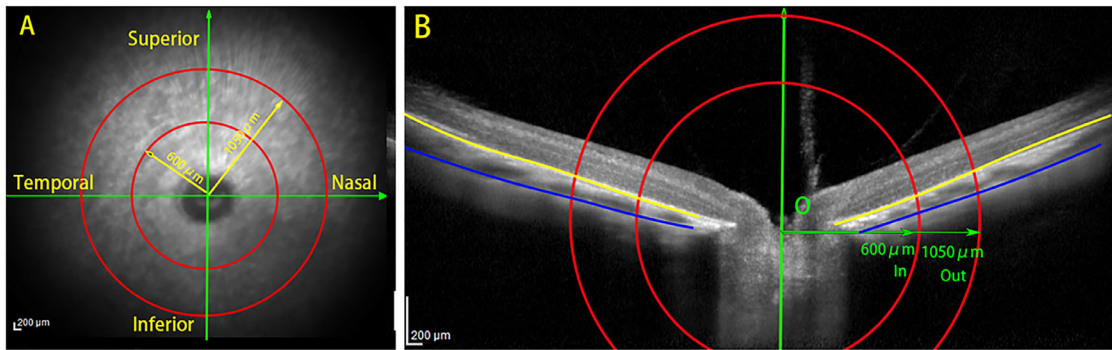
FIGURE 1. Illustration of the measurement of ChT. (**A**) OCT fundus analysis template of guinea pigs. (**B**) Structural images captured by OCT showed the structure of the defined region; the *red lines* represent the inner concentric circle (600 µm, *green arrow*) and outer concentric circle (1050 µm, *green arrow*). The optic disc was defined as the circle center, and the region of interest in each quadrant was located between the border of the choroidal layer and the two *striped green lines*.

TABLE. Primer Sequences for Target Genes

Gene		Primer Sequences
GAPDH	Forward:	5′- CTG ACC TGC CGC CTG GAG AAACC -3′
	Reverse:	5′- ATG CCA GCC CCA GCG TCA AAAGT -3′
RASA1	Forward:	5′- CAA TTC GCC GTA AAA CAA AGG ATG -3′
	Reverse:	5′- CCC GCG AAG TAG AAG ATG TAG TGC -3′
BAD	Forward:	5′- GGA GGC ACT GTG GCT ATG GAG ACC -3′
	Reverse:	5′- AGC GGC CCC GGA ATG GAC TGAGC -3′
BCL-2	Forward:	5′- CTC CCG CCG CTA TCG CCA AGACT -3′
	Reverse:	5′- GAC CCC ACC GAA CTC AAA GAAGG -3′

epithelium, and the lower boundary was the inner surface of the sclera. The optic disc was the center referred to by Zhang et al.,[25] who made two concentric circles with radii of 600 µm and 1500 µm. We also measured the ChT by choosing the area around the intersection of the two concentric circles with the yellow line, and the averaged ChT was from eight locations of four quadrants. In each guinea pig, eight locations were selected for measurements within the four quadrants of superior, inferior, temporal, and nasal sections that intersected the concentric circles, and the average was calculated. We then performed correlation analysis between the axis length and ChT.

Real-Time Fluorescent Quantitative PCR

Choroidal tissues from 2- and 4-week-old NC and LIM guinea pigs were extracted and frozen in liquid nitrogen. Then, equal amounts of choroidal tissues were taken and ground separately using a modified tissue/cellular RNA rapid extraction kit (SparkJade Science Co., Ltd., Jinan, China) to extract total RNA. The RNA purity and concentration were measured by an ultraviolet spectrophotometer (K5600; Beijing Kaiao Technology Development Co., Ltd., Beijing, China). The HiScript II Q RT SuperMix for qPCR (+gDNA wiper) (Vazyme Biotech Co., Ltd., Nanjing, China) was used for reverse transcription to obtain the cDNA of the target genes *RASA1*, BCL-2-associated agonist of cell death (*BAD*), and B-cell lymphoma 2 (*BCL-2*). The cDNA of the above-mentioned target genes was used to perform real-time quantitative PCR (qPCR) with ChamQ Universal SYBR qPCR Master Mix (Vazyme Biotech Co., Ltd.) in 96-well plates (NEST Biotechnology, Wuxi, China). The primer sequences are listed in the Table. The qPCR conditions were as follows: 94°C for 5 seconds, 1 cycle; 94°C for 5 seconds, 54°C for 15 seconds, and 72°C for 10 seconds for 45 cycles. The expression level of the target gene in each sample was normalized to the internal reference level of glyceraldehyde 3-phosphate dehydrogenase (GAPDH), and the result was analyzed using the $2^{-\Delta\Delta CT}$ method.[26]

Western Blot Analysis

To investigate the protein levels of the molecules related to the RASA1 signaling pathway, we used western blot assays to determine the RASA1, RAS, BAD, and BCL-2 protein levels in LIM and NC guinea pigs. After 2 and 4 weeks of myopia induction, eight guinea pigs were randomly selected in each group, and the choroidal tissues were isolated. Phenylmethylsulfonyl fluoride–containing radioimmunoprecipitation assay buffer lysate was then added at a mass volume ratio of 10 mg:100 µL. Furthermore, the tissues were fully ground by electric homogenization at 4°C for 120 seconds and centrifuged at 5000 rpm for 5 minutes (NEST Biotechnology), and the supernatants were then collected. In the present study, 10% sodium dodecyl sulfate–polyacrylamide gel electrophoresis (SDS–PAGE) was used to separate the target proteins, and a polyvinylidene difluoride (PVDF) membrane was used for membrane transfer. RASA1 (dilution 1:1000; ABclonal Biotechnology, Wuhan, China), RAS (dilution 1:1000; ABclonal Biotechnology), BAD (dilution 1:500; BIOSS, Beijing, China), and BCL-2 (dilution 1:1000; BIOSS) primary antibodies were incubated with the membranes overnight at 4°C, and then the PVDF membrane-loaded transferred target proteins were incubated with secondary antibodies against RASA1 (dilution 1:1000), RAS (dilution 1:1000), BAD (dilution 1:500), and BCL-2 (dilution 1:1000) for 1 hour at 4°C. Finally, we used the FUSION-FX7 imaging system (Vilber Lourmat, Marne-la-Vallée, France) for development using DAB (Sigma-Aldrich, St. Louis, MO, USA) and quantified results using fusion CAPT software (Vilber Lourmat).

Statistical Analysis

SPSS Statistics 23.0 (IBM, Chicago, IL, USA) was used for statistical analysis. In the current study, a paired *t*-test was performed for each refractive parameter between eyes at different treatment time points, and an independent sample *t*-test was performed for the right eye of the experimental (LIM) group and the ipsilateral eye of the NC group. An
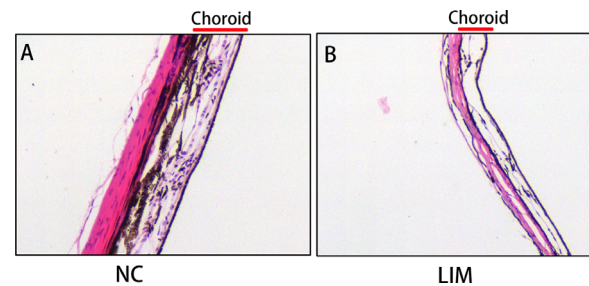
A

B
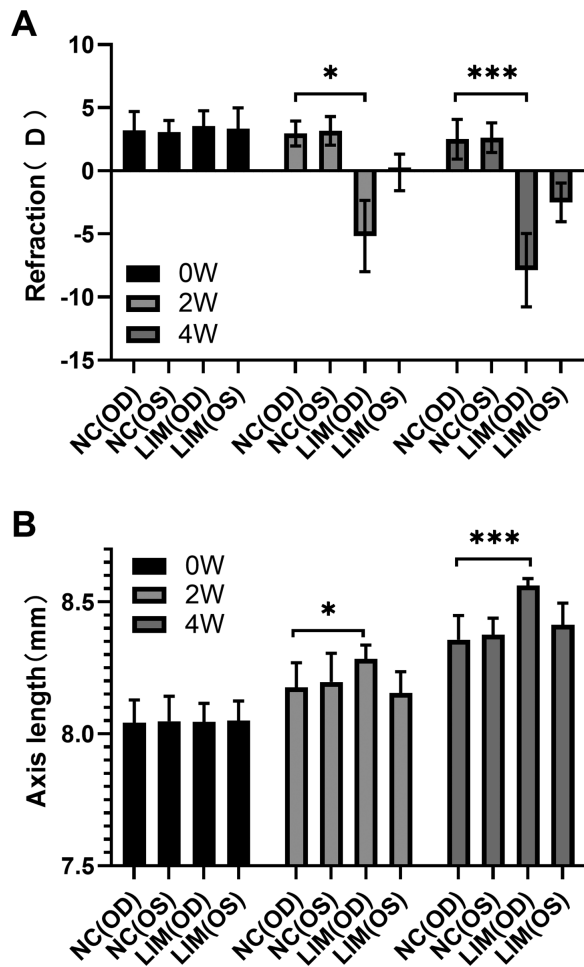
FIGURE 2. The mean values of refraction (**A**) and axial length (**B**) in the left and right eyes of guinea pigs at 0, 2, and 4 weeks were compared between the LIM and NC groups (mean ± SD). LIM represents the negative lens-induced group, and NC represents the normal control group. At 0, 2, and 4 weeks, the LIM group was compared with the NC group (*P < 0.05, **P < 0.01).

FIGURE 3. H&E staining of ocular tissue sections showing histopathological features of the choroid of 4-week-old guinea pigs. The results indicate that the structural arrangement of the choroidal tissue in the NC group was denser and the capillary vascular structure was tighter than that in the LIM group, whereas the structural arrangement within the choroidal stroma of the LIM group was looser, with more obvious fracture dissolution and more sparse vascularity. Magnification, 400×.
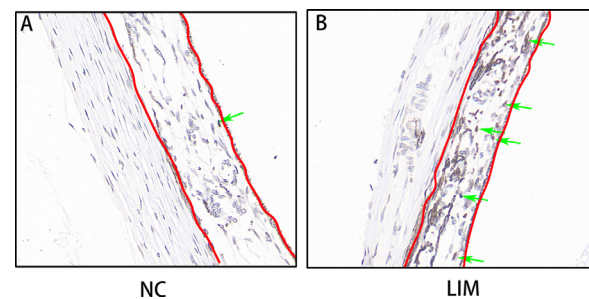
FIGURE 4. TUNEL staining of ocular tissue sections. The TUNEL assay was performed for the LIM guinea pigs after modeling for 4 weeks. The choroidal tissue in the LIM group had more dark brown areas than the NC group and an increased number of TUNEL-positive cells compared to the NC subjects. Magnification, 400×.

independent sample *t*-test was performed for the NC and LIM groups of gene expression. Correlation analysis was used for choroidal thickness and ocular length, and one-way ANOVA was used to analyze the choroidal thickness in the NC and LIM groups. P < 0.05 was considered statistically significant.

RESULTS

Changes in Refraction and Axial Length

We measured the refraction and axial length of both eyes of all guinea pigs prior to myopia induction and found no significant differences between the groups (all P > 0.05). However, after myopia induction for 2 and 4 weeks, we noted that, compared with the self-control (left) eyes in the LIM group and the ipsilateral eyes in the NC group, the refraction of modeled myopic eyes in the LIM group significantly increased (*P < 0.05, ***P < 0.01 in Fig. 2A), and the ocular length was also increased (*P < 0.05, **P < 0.01 in Fig. 2B).

## Pathological Analysis and TUNEL Assay

To investigate the effect of LIM on choroid morphology, we performed H&E staining at 4 weeks after myopia induction. The results showed that the structural arrangement of the choroidal tissues was denser in the NC group, and the capillary vascular structure was more compact. In contrast, the structure of the choroid in the LIM group had a loose arrangement, dissolution was more obvious, and the ChT in the LIM group was significantly thinner than that in the NC group (Fig. 3).

To investigate the apoptosis of choroidal cells in myopic guinea pigs at 4 weeks, we performed TUNEL staining. We noted that, after myopia induction for 4 weeks, the nuclei of hematoxylin-stained cells were blue and the nuclei of positive apoptotic cells revealed by DAB were brownish-yellow. In addition, we also observed an increase in the number of TUNEL-positive cells in the area of darkly stained nuclei in the LIM group compared with the NC group (Fig. 4).

Changes in ChT

Considering that LIM could lead to changes in choroidal morphology, we further measured ChT in guinea pigs before and after myopia induction. As shown in Figure 5, the results indicated that there was no significant difference between the two groups prior to myopia induction (NC, 64.9432 ± 4.6822 µm; LIM, 64.9205 ± 3.01987 µm). However, after myopia induction for 2 and 4 weeks, we found that the ChT
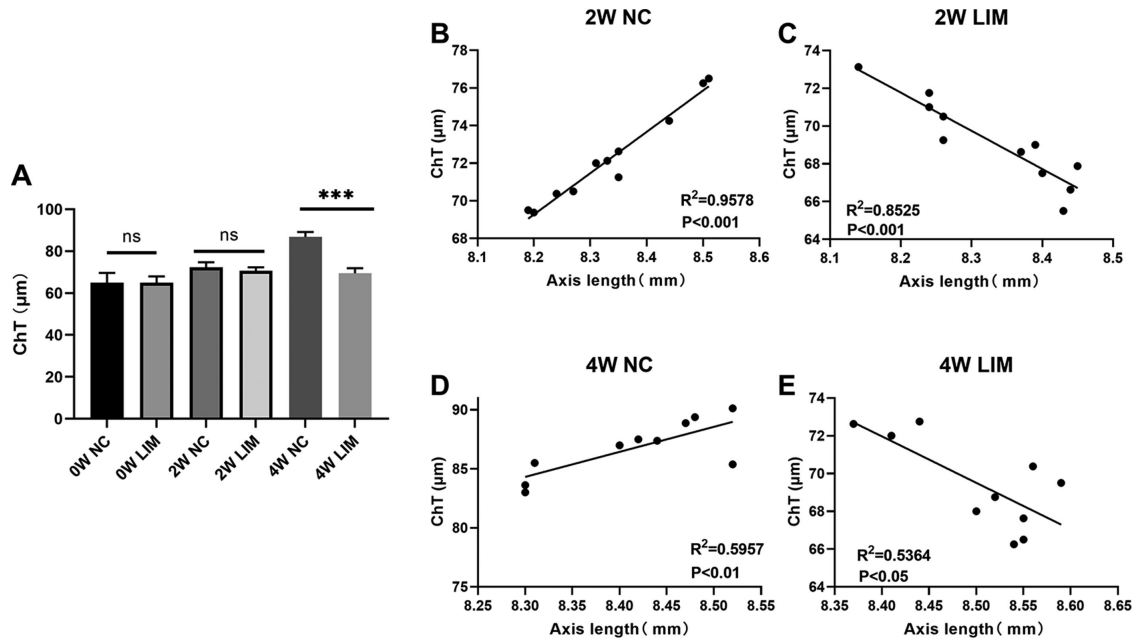
FIGURE 5. Comparison of guinea pig ChT at 0, 2, and 4 weeks. (**A**) Comparison of ChT changes at 2 and 4 weeks. (**B**) Choroidal–ocular axis correlation in the 2-week NC group. (**C**) Choroidal–ocular axis correlation in the 2-week LIM group. (**D**) Choroidal–ocular axis correlation in the 4-week NC group. (**E**) Choroidal–ocular axis correlation analysis in the 4-week LIM group (***$P < 0.001$).
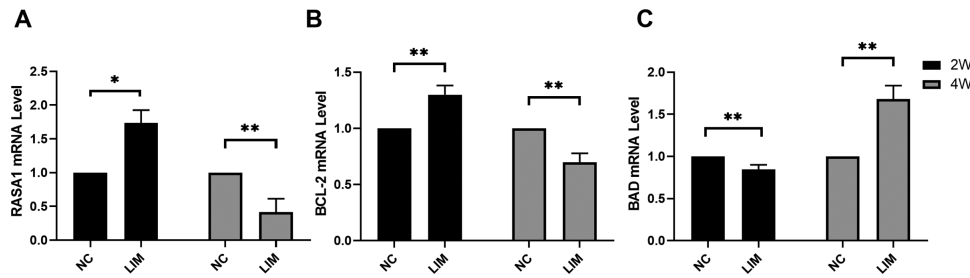
FIGURE 6. The mRNA levels of the *RASA1* (**A**), *BCL-2* (**B**), and *BAD* (**C**) genes in guinea pig choroids were detected by qPCR at 2 weeks and 4 weeks in the NC group and LIM group. *$P < 0.05$ and **$P < 0.01$ in the experimental group compared with the control group.

was significantly reduced in the LIM group (2 weeks: NC, 72.55 ± 2.406 µm; LIM, 70.69 ± 1.590 µm; 4 weeks: NC, 86.29 ± 2.510 µm; LIM, 68.94 ± 4.345 µm; ***$P < 0.001$), demonstrating that the ChT of the LIM guinea pigs showed a negative correlation with axial length (Fig. 5).

RASA1, *BAD*, *RAS*, and *BCL-2* Expression

As shown in Figure 6, qPCR showed that, compared with that in the NC group, *RASA1* gene expression in the LIM group was elevated at 2 weeks after myopia induction and was statistically significant ($P < 0.05$) (Fig. 6A), whereas it decreased at 4 weeks after myopia induction ($P < 0.01$) (Fig. 6A). Similarly, the *BCL-2* level was elevated at 2 weeks and decreased at 4 weeks after myopia induction compared to the NC group (Fig. 6B). In contrast, the *BAD* gene levels were reduced at 2 weeks and increased at 4 weeks after myopia induction compared with the NC group (Fig. 6C).

Consistent with *RASA1*, *BAD*, *RAS*, and *BCL-2* gene expression, Figure 7 indicates that RASA1, RAS, and BCL-2 protein expression levels were upregulated at 2 weeks

after myopia induction and downregulated at 4 weeks after myopia induction compared with the NC group. In contrast, the BAD protein level was reduced at 2 weeks and increased at 4 weeks after myopia induction compared with the NC group; therefore, we may infer that the aberrant expression of BCL-2 and BAD will activate apoptotic signaling and induce the apoptosis of choroid-related cells, and the increment of apoptotic cells is related to choroidal thinning.

DISCUSSION

In this study, we found that RASA1 regulates the expression of RAS, BAD, and BCL-2 in the downstream molecules of the RASA1 signaling pathway and that RASA1-regulated downstream molecules showed different expression trends in the choroid tissues of myopic guinea pigs at 2 weeks and 4 weeks. Meanwhile, the OCT angiography results showed that the ChT of guinea pigs in the LIM group showed an attenuated trend. We speculate that the varying levels of RASA1 at different time points could be attributed to the state of cellular growth and the stress levels in guinea pigs
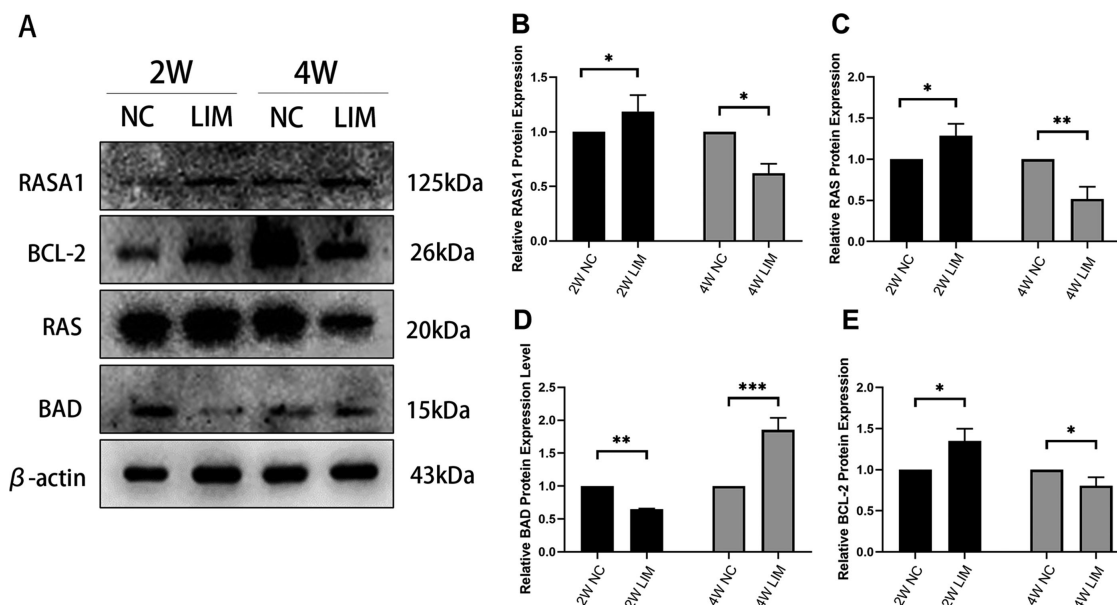
FIGURE 7. Western blot analysis of RASA1, RAS, BAD, and BCL-2. (**A**) Relative levels of the choroidal target proteins RASA1 (**B**), RAS (**C**), BAD (**D**), and BCL-2 (**E**) in guinea pigs in the NC and LIM groups at 2 and 4 weeks, with β-actin as an internal reference. For the comparison between LIM and NC groups, $^*P < 0.05$, $^{**}P < 0.01$, and $^{***}P < 0.001$.

induced by LIM. This would decrease cell viability in the choroid, influence the normal physiological function, and affect the growth and development of choroidal vessels, which would impact the ChT of guinea pigs and aggravate myopia.

Current research on RASA1 signaling is mostly limited to cancer and other diseases,[27] and little research has concentrated on myopia. It has been shown that microRNAs can regulate expression of the *RASA1* gene and thus play a role in myocardial fibrosis and vascular lymphatic vessel development, in addition to driving the cellular output of type IV collagen to control the development of lymphatic veins and venous valves in mice[28,29]; therefore, we propose that there is a close relationship between RASA1 signaling and ChT development. The choroid is mainly composed of blood vessels and lymphatic tissue, and studies have shown that RASA1 and its downstream molecules affect blood vessel growth and development.[27] Thus, in the present study, we performed relevant experiments to explore the relationship between the expression levels of RASA1 signaling-related molecules and ChT in LIM guinea pigs. We demonstrated that RASA1 showed high expression at 2 weeks after myopia induction and low expression at 4 weeks after myopia induction. RASA1 is a regulator of GTP and RAS GTP, which are involved in multiple physiological processes, including angiogenesis, cell proliferation, and apoptosis.[18] It has been reported that overexpression of RASA1 can suppress cell growth and promote apoptosis.[30] Moreover, RASA1 signaling governs multiple downstream molecules, including BCL-2, BAD, and RASA1, which are also associated with the apoptotic signaling pathway. In this study, we noted that BCL-2 was highly expressed at 2 weeks after myopia induction and was expressed at low levels at 4 weeks after myopia induction.

Cellular stress is sensed by a few molecules and pathways that can stimulate either cell survival or apoptosis, and the stress response depends on the degree of stimulation or molecule-mediated differential posttranslational modifi-

cations.[32] RASA1, also known as p120 RasGAP, is a regulator of RAS guanosine diphosphate and GTP. It is regarded as a signaling scaffold protein, playing a vital role in anti-apoptotic and cell death-inducing effects and relying on activation of the fragment C and fragment N split from RasGAP.[32] Fragment N can activate the anti-apoptotic response and inhibit apoptosis when the organism suffers from mild stress. However, if the organism is suffering from strong stress, fragment C would be activated to induce apoptosis, ultimately leading to cell death,[33] suggesting that the organism can regulate cellular function, the microenvironment, and organism homeostasis through stress responses.[34,35] Nevertheless, stress responses may diminish over time when external stimuli persist; hence, cells will eventually die under constant intense stress due to the limitation of the stress response.

In the present study, we found that RASA1 expression was significantly elevated at 2 weeks of myopia induction to promote survival. In contrast, RASA1 expression decreased significantly at 4 weeks after myopia induction, accompanied by elevated apoptosis of choroidal cells and significant thinning of choroidal thickness. Based on the experimental results, we hypothesize that, during the early phase of myopia induction (in the first 2 weeks), external stimulation serves as a mild stressor and will activate the anti-apoptotic response, thereby inhibiting apoptosis. As myopia induction continues (after myopia induction for 4 weeks), the external stimulus turns into a strong stressor, which activates the apoptotic response, leading to apoptosis (Fig. 8).

BCL-2 plays an anti-apoptotic role that normally induces the formation of mitochondrial pores by inhibiting apoptosis,[36,37] thereby preventing the release of cytochromes from mitochondria.[38] It has been reported that mitochondria are closely associated with protein synthesis; meanwhile, as power-generated organelles, they can also generate chemical energy (adenosine triphosphate). In addition, mitochondrial dysfunction is also correlated with neurodegenerative diseases and the aging process,[39] and these
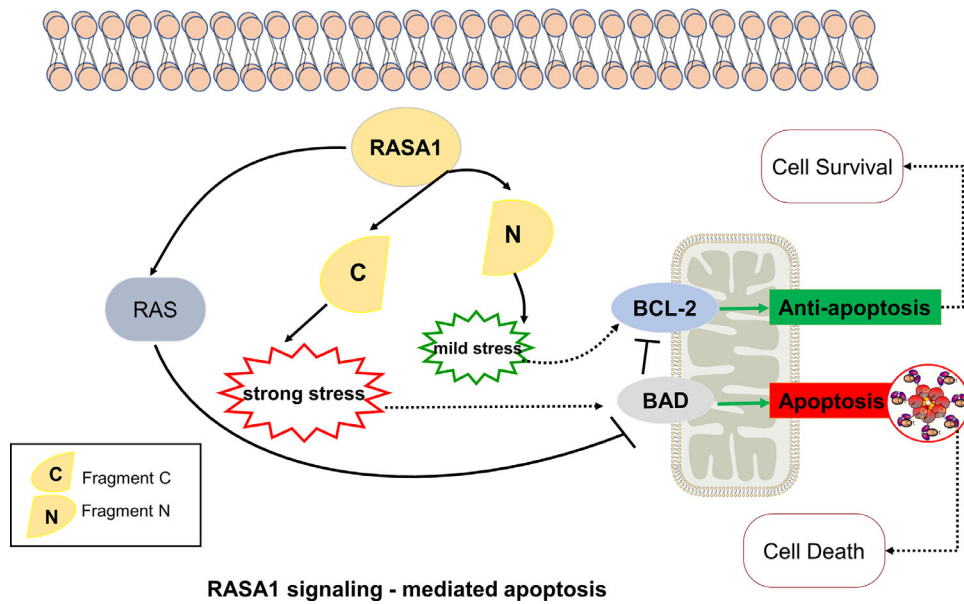
FIGURE 8. The RASA1 signaling pathway mediates apoptosis. RASA1 signaling has anti-apoptotic and cell death-inducing effects. The specific mechanism of action leads to the partial cleavage of RasGAP into fragment C and fragment N. When an organism suffers from mild stress, fragment N activates BCL-2, which generates an anti-apoptotic response and inhibits the further response to apoptosis. However, when an organism suffers from stronger stress, fragment C will be activated, leading to an apoptotic response in the downstream BAD and cell death.

diseases are closely related to RASA1 signaling. The choroid is rich in blood vessels and is the major blood supply to the retina because the retinal photoreceptors are extremely metabolically active.[12] In this study, we found that, after myopia induction for 2 weeks, sparse vascularization of the choroidal tissue in guinea pigs occurred due to the presence of negative lens induction, resulting in sustained high expression of RASA1 (Fig. 3), leading to low expression of the downstream signaling molecule BCL-2 as well as elevated BAD and thus mediating apoptosis. When myopia induction proceeded (4 weeks after myopia induction), the expression levels of RASA1 decreased, affecting BCL-2 expression and thereby promoting apoptosis.

In this study, although we found no significant difference in the choroidal thickness between the NC and LIM groups at 2 weeks, there was a statistically significant difference between the two groups after myopia induction for 4 weeks, and this result is also consistent with the gene expression profile. We further confirmed a negative correlation between ChT and ocular length in the LIM group. According to the literature,[40,41] there is a strong correlation between ChT and choroidal blood perfusion in guinea pigs. A relevant study done in humans confirmed a significant decrease in ChT in highly myopic patients.[42] There is a significant correlation between ChT and ocular length,[43] and ChT also appears to decrease significantly in children in the early stages of myopia.[44] In our study, the ChT of guinea pigs in the LIM group was consistent with the results of the literature. We also found that there was a negative correlation between ChT and vessel density of the choriocapillaris with the development of myopia.[45]

The initiation of the RASA1 signaling pathway and the low expression of the downstream BCL-2 result in choroidal cell apoptosis, thus leading to a decrease in ChT. With the decrease in ChT, the rapid change in the choroid makes the retina move back, allowing objects to fall out of the retina.[12] In this case, myopia progression reduced the ChT

in LIM guinea pigs, thus resulting in an increased ocular length.

Nevertheless, the current study still has limitations. First, pharmacological manipulations are required at the basic level to establish a relationship between RASA1 and apoptosis, which is missing in this study. In addition, whether the choroid influences the function of the retina and sclera and thus regulates the development of myopia is still unclear. Although we could not define the specific type of apoptosis, we propose new avenues to explore the pathogenesis of myopia.

CONCLUSIONS

In summary, we confirmed that choroidal thickness gradually decreased in guinea pigs with negative lens-induced myopia, which was accompanied by a negative correlation with ocular length. We also noted that negative lens-induced myopia can cause activation of the RASA1 signaling pathway and apparently lead to low expression of BCL-2 and elevated expression of BAD, initiating an apoptotic pathway and thereby leading to apoptosis of choroidal tissue-related cells and a decrease in choroidal thickness. In conclusion, the increased number of apoptotic cells in choroidal tissues mediated by myopia drives the decrease in choroidal thickness. Our findings indicate that the activation of RASA1 signaling can induce the apoptosis of choroidal cells that reduce choroidal thickness and may be a new target in the treatment of myopia.

References

1. Morgan IG, Ohno-Matsui K, Saw SM. Myopia. *Lancet*. 2012;379(9827):1739–1748.

2. Morgan IG, French AN, Ashby RS, et al. The epidemics of myopia: aetiology and prevention. *Prog Retin Eye Res*. 2018;62:134–149.

3. Priscilla JJ, Verkicharla PK. Time trends on the prevalence of myopia in India–a prediction model for 2050. *Ophthalmic Physiol Opt*. 2021;41(3):466–474.

4. He M, Xiang F, Zeng Y, et al. Effect of time spent outdoors at school on the development of myopia among children in China: a randomized clinical trial. *JAMA*. 2015;314(11):1142–1148.

5. Yang GY, Huang LH, Schmid KL, et al. Associations between screen exposure in early life and myopia amongst Chinese preschoolers. *Int J Environ Res Public Health*. 2020;17(3):1056–1056.

6. Wang SK, Guo Y, Liao C, et al. Incidence of and factors associated with myopia and high myopia in Chinese children, based on refraction without cycloplegia. *JAMA Ophthalmol*. 2018;136(9):1017–1024.

7. Wang J, Ying GS, Fu X, et al. Prevalence of myopia and vision impairment in school students in Eastern China. *BMC Ophthalmol*. 2020;20(1):2.

8. Cooper J, Tkatchenko AV. A review of current concepts of the etiology and treatment of myopia. *Eye Contact Lens*. 2018;44(4):231–247.

9. Cai XB, Shen SR, Chen DF, Zhang Q, Jin ZB. An overview of myopia genetics. *Exp Eye Res*. 2019;188:107778.

10. Piao H, Guo Y, Zhang H, Sung MS, Park SW. Acircularity and circularity indexes of the foveal avascular zone in high myopia. *Sci Rep*. 2021;11(1):1–10.

11. Singh SR, Vupparaboina KK, Goud A, Dansingani KK, Chhablani J. Choroidal imaging biomarkers. *Surv Ophthalmol*. 2019;64(3):312–333.

12. Nickla DL, Wallman J. The multifunctional choroid. *Prog Retin Eye Res*. 2010;29 (2):144–168.

13. Margolis R, Spaide RF. A pilot study of enhanced depth imaging optical coherence tomography of the choroid in normal eyes. *Am J Ophthalmol*. 2009;147(5):811–815.

14. Quintela T, Furtado A, Duarte AC, Goncalves I, Myung J, Santos CRA. The role of circadian rhythm in choroid plexus functions. *Prog Neurobiol*. 2021;205:102129.

15. Summers JA. The choroid as a sclera growth regulator. *Exp Eye Res*. 2013;114:120–127.

16. Hershkovitz D, Bergman R, Sprecher E. A novel mutation in RASA1 causes capillary malformation and limb enlargement. *Arch Dermatol Res*. 2008;300(7):385–388.

17. Li X, Li D, Wikstrom JD, et al. MicroRNA-132 promotes fibroblast migration via regulating RAS p21 protein activator 1 in skin wound healing. *Sci Rep*. 2017;7(1):7797.

18. Zhang Y, Li Y, Wang Q, et al. Role of RASA1 in cancer: a review and update (review). *Oncol Rep*. 2020;44(6):2386–2396.

19. Gallipoli A, MacLean G, Walia JS, Sehgal A. Congenital chylothorax and hydrops fetalis: a novel neonatal presentation of RASA1 mutation. *Pediatrics*. 2021;147(3):e2020011601.

20. Pan M, Zhao F, Xie B, et al. Dietary ω-3 polyunsaturated fatty acids are protective for myopia. *Proc Natl Acad Sci USA*. 2021;118(43):e2104689118.

21. Geng C, Li Y, Guo F, et al. RNA sequencing analysis of long non-coding RNA expression in ocular posterior poles of guinea pig myopia models. *Mol Vis*. 2020;26:117–134.

22. Zhou X, Qu J, Xie R, et al. Normal development of refractive state and ocular dimensions in guinea pigs. *Vision Res*. 2006;46(18):2815–2823.

23. Wu S, Guo D, Wei H, et al. Disrupted potassium ion homeostasis in ciliary muscle in negative lens-induced myopia in Guinea pigs. *Arch Biochem Biophys*. 2020;688:108403.

24. Shkreli M, Sarin KY, Pech MF, et al. Reversible cell-cycle entry in adult kidney podocytes through regulated control of telomerase and Wnt signaling. *Nat Med*. 2011;18(1):111–119.

25. Zhang S, Zhang G, Zhou X, et al. Changes in choroidal thickness and choroidal blood perfusion in guinea pig myopia. *Invest Ophthalmol Vis Sci*. 2019;60(8):3074–3083.

26. Livak KJ, Schmittgen TD. Analysis of relative gene expression data using real-time quantitative PCR and the $2^{-\Delta\Delta CT}$ method. *Methods*. 2001;25:402–408.

27. Zhang RL, Aimudula A, Dai JH, Bao YX. RASA1 inhibits the progression of renal cell carcinoma by decreasing the expression of miR-223-3p and promoting the expression of FBXW7. *Biosci Rep*. 2020;40(7):BSR20194143.

28. Liu X, Xu Y, Deng Y, Li H. MicroRNA-223 regulates cardiac fibrosis after myocardial infarction by targeting RASA1. *Cell Physiol Biochem*. 2018;46(4):1439–1454.

29. Chen D, Geng X, Lapinski PE, Davis MJ, Srinivasan RS, King PD. RASA1-driven cellular export of collagen IV is required for the development of lymphovenous and venous valves in mice. *Development*. 2020;147(23):dev192351.

30. Jing L, Li H, Zhang T, Lu J, Zhong L. MicroRNA 4530 suppresses cell proliferation and induces apoptosis by targeting RASA1 in human umbilical vein endothelial cells. *Mol Med Rep*. 2019;19(5):3393–3402.

31. McCullough KD, Martindale JL, Klotz LO, Aw TY, Holbrook NJ. Gadd153 sensitizes cells to endoplasmic reticulum stress by down-regulating Bcl2 and perturbing the cellular redox state. *Mol Cell Biol*. 2001;21(4):1249–1259.

32. Khalil H, Bertrand MJ, Vandenabeele P, Widmann C. Caspase-3 and RasGAP: a stress-sensing survival/demise switch. *Trends Cell Biol*. 2014;24(2):83–89.

33. Yang JY, Widmann C. Antiapoptotic signaling generated by caspase-induced cleavage of RasGAP. *Mol Cell Biol*. 2001;21(16):5346–5358.

34. Galluzzi L, Yamazaki T, Kroemer G. Linking cellular stress responses to systemic homeostasis. *Nat Rev Mol Cell Biol*. 2018;19(11):731–745.

35. Fuchs Y, Steller H. Live to die another way: modes of programmed cell death and the signals emanating from dying cells. *Nat Rev Mol Cell Biol*. 2015;16(6):329–344.

36. Wei Y, Pattingre S, Sinha S, Bassik M, Levine B. JNK1-mediated phosphorylation of Bcl-2 regulates starvation-induced autophagy. *Mol Cell*. 2008;30(6):678–688.

37. Tao SC, Yuan T, Rui BY, Zhu ZZ, Guo SC, Zhang CQ. Exosomes derived from human platelet-rich plasma prevent apoptosis induced by glucocorticoid-associated endoplasmic reticulum stress in rat osteonecrosis of the femoral head via the Akt/Bad/Bcl-2 signal pathway. *Theranostics*. 2017;7(3):733–750.

38. Zhang L, Wang K, Lei Y, Li Q, Nice EC, Huang C. Redox signaling: potential arbitrator of autophagy and apoptosis in therapeutic response. *Free Radic Biol Med*. 2015;89:452–465.

39. Kummer E, Ban N. Mechanisms and regulation of protein synthesis in mitochondria. *Nat Rev Mol Cell Biol*. 2021;22(5):307–325.

40. Zhou X, Zhang S, Zhang G, et al. Increased choroidal blood perfusion can inhibit form deprivation myopia in guinea pigs. *Invest Ophthalmol Vis Sci.* 2020;61(13):25.

41. Zhou X, Zhang S, Yang F, et al. Decreased choroidal blood perfusion induces myopia in guinea pigs. *Invest Ophthalmol Vis Sci.* 2021;62(15):30.

42. Zhang JM, Wu JF, Chen JH, et al. Macular choroidal thickness in children: the Shandong Children Eye Study. *Invest Ophthalmol Vis Sci.* 2015;56(13):7646–7652.

43. Liu B, Wang Y, Li T, et al. Correlation of subfoveal choroidal thickness with axial length, refractive error, and age in adult highly myopic eyes. *BMC Ophthalmol.* 2018;18(1): 127.

44. Prousali E, Dastiridou A, Ziakas N, Androudi S, Mataftsi A. Choroidal thickness and ocular growth in childhood. *Surv Ophthalmol.* 2021;66(2):261–275.

45. Yu T, Xie X, Wei H, et al. Choroidal changes in lens-induced myopia in guinea pigs. *Microvasc Res.* 2021;138:104213.